



LHCb-PUB-2015-012

02/07/2015

*LHCb SciFi project*

# An experimental set-up to measure Light Yield of Scintillating Fibres

C. Alfieri<sup>1)</sup>, A.B. Cavalcante<sup>2)</sup>, C. Joram<sup>1)</sup>, M. W. Kenzie<sup>1)</sup>

<sup>1)</sup> CERN / PH Department

<sup>2)</sup> Centro Brasileiro de Pesquisas Físicas (CBPF), Rio de Janeiro, Brazil

## *Abstract*

In the context of the LHCb SciFi Tracker project, an experimental set up was designed and built to provide reliable and reproducible measurements of the light yield of scintillating fibres.

This document describes the principle and technical realisation of the set-up. A few examples illustrate the operation and data analysis.

In the first implementation of the set-up a photomultiplier tube with bialkali photocathode was used for the reading of the light from the fibres under test. In order to measure also green emitting fibres, the photomultiplier was replaced in January 2016 by a SiPM with higher sensitivity and larger spectral coverage<sup>1</sup>.

---

<sup>1</sup> The upgraded set-up is described in sec.5, added to this note in January 2016.

## 1. Introduction

Scintillating plastic fibres are considered as active detector elements in the SciFi tracker project [15]. While the scintillating fibre technology is well established and its performance can be considered as proven, the particular conditions of the upgraded LHCb detector at the Large Hadron Collider pose stringent requirements on a variety of aspects.

The SciFi tracker will consist of 12 detector planes of  $4.8 \times 6 \text{ m}^2$  size, placed to the LHC beam axis. A plane will be made of 6 layers of  $250 \mu\text{m}$  thick fibres, hexagonally packed into mats. In a plane, the fibres are oriented vertically or with an angle of  $\pm 5$  degrees relative to the vertical direction (stereo planes). For technical reasons, the planes will be subdivided in smaller identical units. For what concerns the fibres, the base unit is conceived to be 2.4 m long and 13 cm wide. The full detector will consist of 1152 base units, which leads to a total fibre length of about 10'000 km. One end of the fibre will be read out by SiPM photodetectors. The non-read end is mirrored in order to maximise the quantity of detectable light.

The hit efficiency of the SciFi tracker depends crucially on the number of photons which can be detected at the end of the fibre. One parameter which drives this number is the intrinsic scintillation yield.

Signal generation in a scintillating fibre is a multi-step process. Ionisation energy deposited in the core of the fibre leads to excitation of molecular levels (specifically of the so-called  $\pi$  electrons) in the benzene rings of the polymer chain. The relaxation time and scintillation light yield of polystyrene are however poor. An organic fluorescent dye with matched excitation energy levels is added to the polystyrene base ( $\sim 1\%$  by weight) to improve the efficiency of the scintillation mechanism. Energy is transferred quite rapidly (sub-ns) from the base to this 'activator' dye by means of a non-radiative dipole-dipole transmission, known as the Förster transfer, where the excited energy state of the dye will subsequently relax by emission of a photon. The activator dye is chosen to have a high quantum efficiency ( $> 95\%$ ), a particular emission wavelength spectra, and fast decay time (less than a few ns). Often, a second wavelength shifting dye is admixed ( $\sim 0.05\%$  by weight) which absorbs the photons from the activator (blue or UV) and remits them (isotropically) at longer wavelength (blue-green). At longer wavelength, the probability of reabsorption by the dyes is reduced and the photons profit from a generally better transparency of the polystyrene.

The intrinsic scintillation yield of a fibre, describing the number of photons emitted by the wavelength shifting dye normalised to a given energy deposition, usually 1 MeV, is difficult to measure. In addition, it is to a certain extent depending on the diameter of the fibre as primary photons may escape from a thin fibre un-shifted. Some producers provide the yield figure of 7000 – 8000 photons per MeV.

For the purpose of comparing different fibres or monitoring their quality during the phase of series production, it is sufficient to measure an effective light yield under defined and stable experimental conditions. Excitation of the fibre by an ionising particle or an x-ray photon is however mandatory. The ionising radiation cannot be replaced by UV light as this would just excite the wavelength shifting dye without assessing the scintillation process itself.

In the following, we describe a set-up which allows measuring the detected light output, in units of photoelectrons, created by a minimum ionising particle. The measurement is related to the intrinsic

scintillation yield by a constant but unknown factor, which can in principle be obtained by modelling the full set-up.

## 2. The experimental set-up

The set-up is conceived to measure the light yield, in photoelectrons, detected at the end of a fibre following energy deposition by a minimum ionising particle at a given position from the photodetector (Signal PMT). Figure 1 shows the main components of the set-up and the arrangements of the fibres.

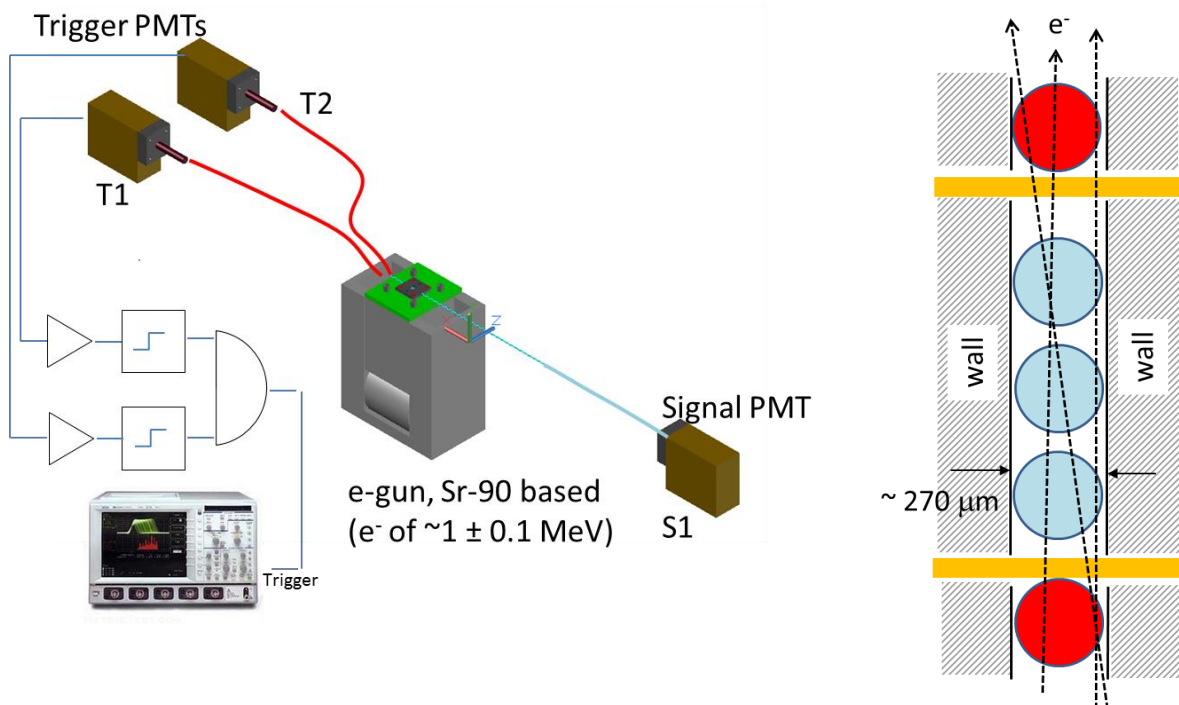


Figure 1 : Left: Main components of the scintillation yield set-up. Right: Details of the arrangement of the trigger fibre (top and bottom in red) and the fibres under test in between.

The light yield of a single scintillation fibre of 250 μm diameter is small and therefore difficult to discriminate from noise which is inherent to any set-up. We therefore read the combined signal of several fibres with a single photodetector. Three fibres have proven a good compromise between sufficiently high signal amplitude and mountability.

As shown on the right hand side of Figure 1, the fibres under test are vertically piled up in a channel between two plastic walls and sandwiched between two trigger fibres, which have also a diameter of 250 μm. Thinn sheets of opaque plastic serve as optical separation between the trigger fibres and the fibres under test (FUT). The length of the fibres between the excitation point (e-gun) and the photodetector (see below) can be varied.

The two trigger fibres are individually read by photomultiplier tubes (PMT) of type Hamamatsu H7826. For the readout of very weak light signals at a low rate, photomultiplier tubes provide a significant advantage over SiPM detectors. Their dark noise rate at the 1 photoelectron level is several orders of magnitude lower than that of a SiPM. This allows setting low thresholds (approx. 1 p.e.) to the trigger counters without generating any random coincidences.

For the joint readout of the 3 FUTs we have two options: a PMT of the same type as the trigger PMTs (H7826) or, as implemented since January 2016, a SiPM detector. The main goal was to overcome the poor quantum efficiency of the bialkali photocathode in the green part of the spectrum. This region is particularly interesting for new green-emitting NOL fibres. The details of the SiPM readout are discussed in section 5.

### Operation and data acquisition

Quasi-minimum ionising particles are provided by an energy filtered Sr-90 source described below in more detail. A trigger signal is generated from the AND of the amplified (x10) and discriminated signals of the two trigger PMTs. The acquisition of the FUT signal, either from the PMT or the SiPM, is based on a digital oscilloscope Lecroy LT344 which samples the voltage pulse in a window of interest. Integration of the signal leads to the corresponding signal charge, which following appropriate calibration, is expressed in photoelectrons.

Figure 2 shows a photo of the part of the set-up which is located in a dark room, while the electronics is located in the illuminated sector of the lab.

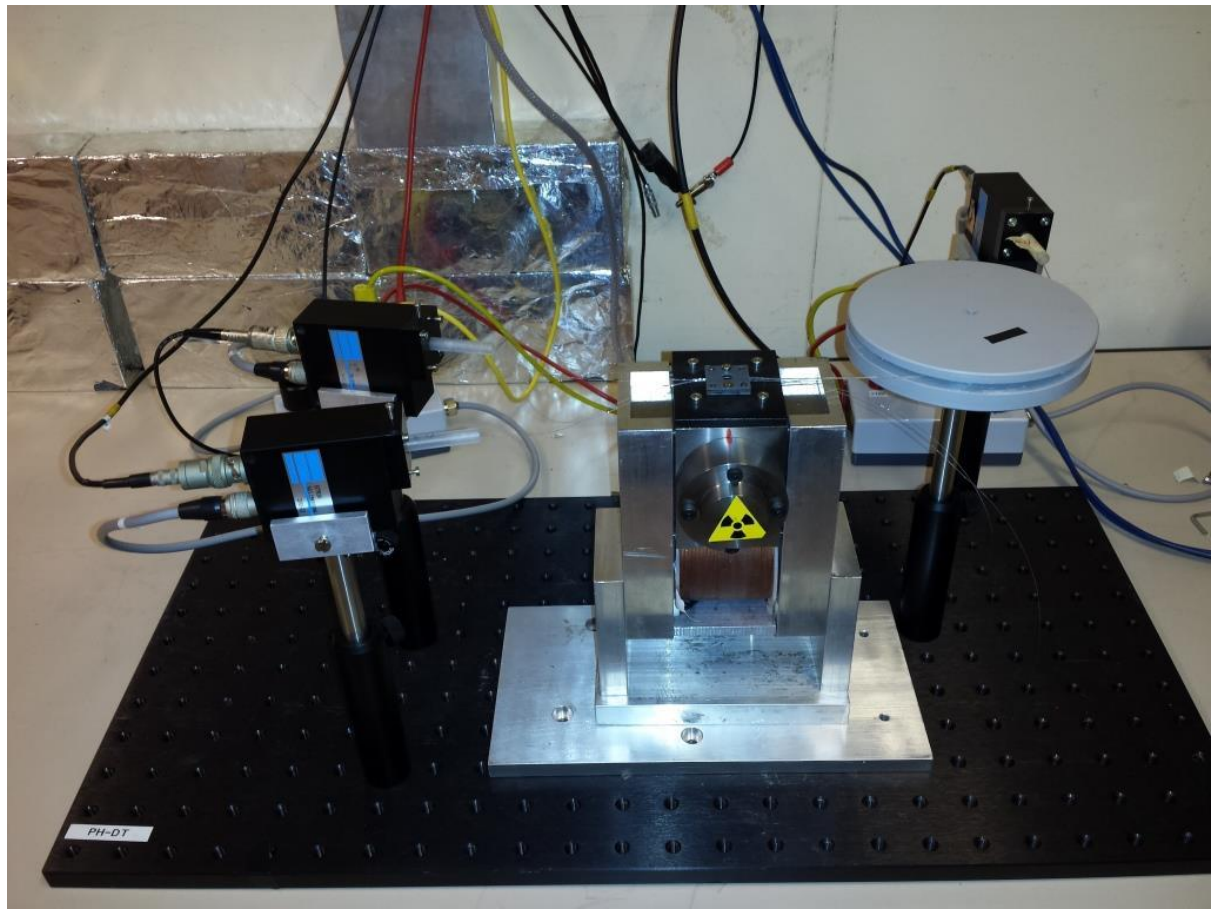


Figure 2 : Photo of the experimental set-up. The grey spool on the right hand side of the e-gun, takes up the excess length of the fibre under test. One turn corresponds to 30 cm fibre length.

### 2.1 The Sr-90 source and electron monochromator

The so-called electron gun, see Figure 3, consists of an intense Sr-90 electron source ( $\varnothing$  1 mm, 370 MBq) mounted inside a simple magnetic monochromator. The body of the monochromator is made of Tungsten. Two collimators and the magnetic field of an electro magnet select a momentum window

from the continuous  $\beta$  spectrum of the source, which has two components: the decay of Sr-90 releases an electron of up to 546 keV, and the decay of the daughter nucleus Y-90 generates an electron of up to 2.27 MeV. The cavity of the tungsten body through which the electrons fly lies only in the return field region of the magnet. Lateral soft iron inserts ensure that the return field is intensified in this region.

The magnetic field in the cavity has been measured by means of a small Hall probe. The results are shown in Figure 4. An identical electron gun has previously been used and absolutely calibrated in energy [1]. Based on these results we chose a magnet current of 0.7 A which provides a field of 3000 kG (0.3 T) and selects electrons of  $1.1 \pm 0.1$  MeV kinetic energy. Such electrons are minimum ionising, i.e. their differential energy loss in plastic scintillator is about 2 MeV/cm.

The energy selection and the collimation by the tungsten slits leads to a large reduction of the source intensity. Furthermore the size of the trigger counters defines only a small solid angle. Typical trigger rates are of the order 10-20 Hz. At the chosen energy, the rate of the source reaches a maximum.

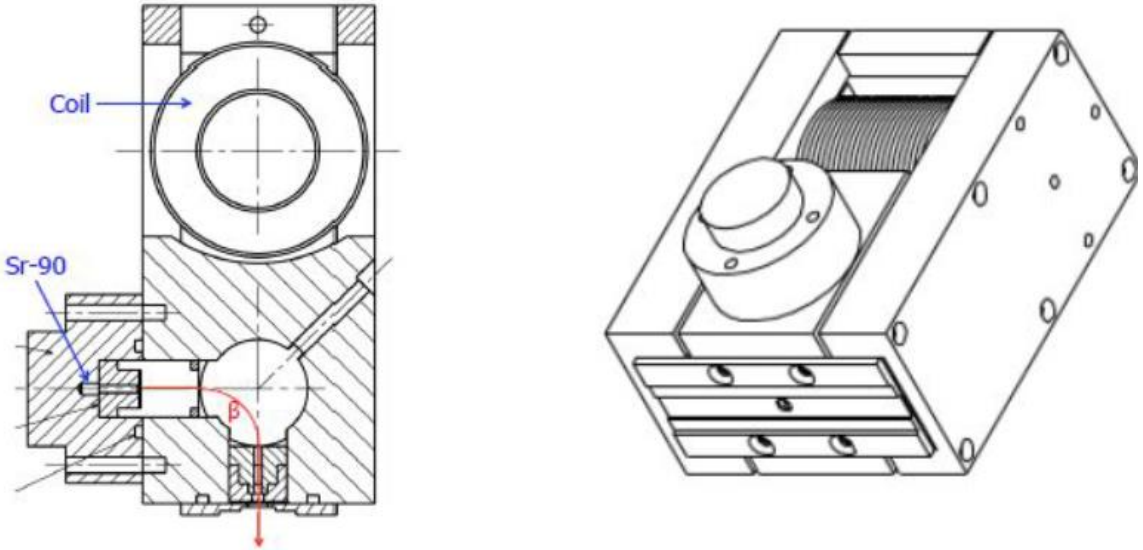


Figure 3: Side and 3D view of the electron gun.

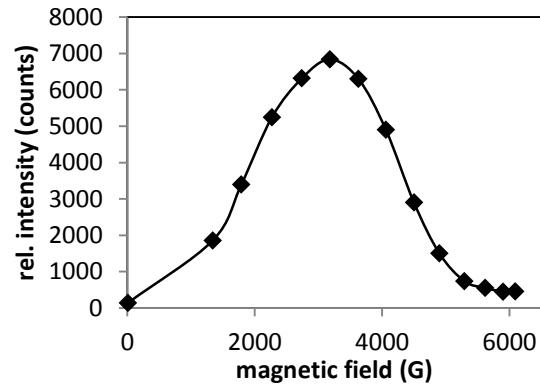
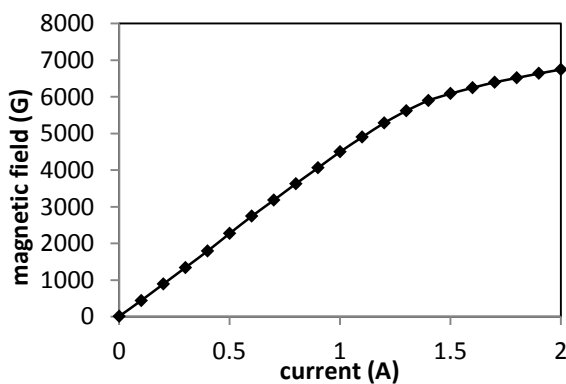


Figure 4: E-gun characterisation. Magnetic field vs. current through the magnet coil.

Figure 5: E-Gun characterisation. Rate vs. magnetic field.

## 2.2 Details of the fibre preparation and positioning

The light yield of a single fibre ( $\phi$  0.25mm) is low and difficult to discriminate from background, particularly for long distances between the excitation and detection points. The set-up was therefore conceived to allow for a vertical stacking of up to 4 fibres to be measured with two additional trigger fibres, one below and one above. The mechanics must on one hand provide a precise alignment of the fibres and avoid any damage while mounting or moving the fibres, on the other.

It consists of two identical square pieces with a longitudinal 0.25mm groove and four precision holes. They hold the trigger fibres. The FUT are held between two identical rectangular pieces, 1mm thick, with two precision holes: When they are mounted on the stack (and upholstered with a 40-micrometer thick kapton layer) they leave between them a gap of 0.27mm width in which the up to 4 FUT can be mounted. Mounting 4 fibres has proven tedious and bears a risk of damage to the fibres. A set of 3 fibres is therefore the default. The optical separation between trigger and signal fibres is provided by a 40  $\mu$ m kapton layer. Precision pins ( $\phi$  3mm) ensure correct stacking and two screws gently squeeze the complete structure which is in turn aligned w.r.t. the exit slit of the monochromator.

We measure the light yield at different distances between the excitation and detection points. The excess fibre lengths, on either side of the excitation point, are enrolled on disks of 30 cm circumference. This provides proper fibre arrangement and at the same time reproducible excitation points. We estimate the uncertainty in the distance to be better than 2 cm.

The amount of light leaving the fibres depends also on the quality of the fibre end cut. In order to have also here reproducible conditions, the ends of the FUT are (jointly) glued into a cylindrical plastic endpiece using fast hardening epoxy glue (Araldite rapid). The endpiece has a central hole of 0.7 mm, which centres the (3) fibres. After full hardening, the end piece is machined by a special fibre polishing machine<sup>2</sup> based on a diamond tool. The coupling to the photodetector, be it PMT or SiPM, is without optical grease, and the losses at the fibre-photodetector interface are of the order 9-10 %. The non-read fibre ends are left as cut with a fibre blade cutter.

---

<sup>2</sup> FiberFin, [www.fiberfin.com](http://www.fiberfin.com)

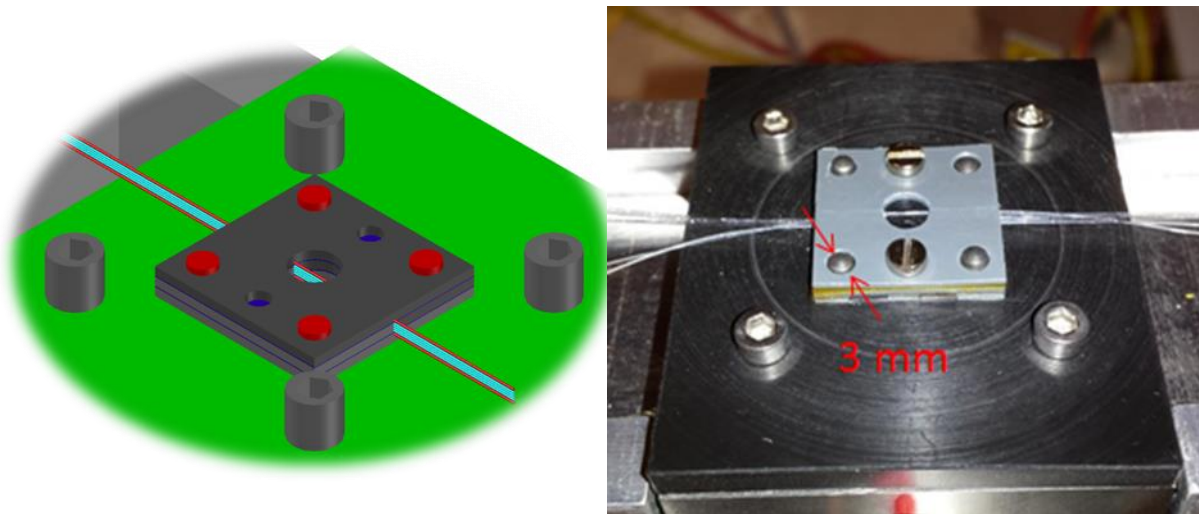


Figure 6 : 3D drawing and photo of the fibre alignment jig.

### 2.3 Single Photoelectron Calibration

The conversion of the photodetector signal charge to photoelectrons relies on the single photoelectron calibration. The chosen PMT type, Hamamatsu H7826, provides high gain (approx.  $10^6$ ) and a decent separation of the single photoelectron distribution from the pedestal peak. The gain of the SiPM is even higher resulting in very narrow charge peaks which allow straightforward photon counting.

#### PMT calibration

The signal charge of a single photoelectron, i.e. the charge gain  $G_{1pe}$ , is determined by exposing the PMT to pulsed low intensity light from a LED. The read-out on the oscilloscope is triggered at every LED pulse. The oscilloscope integrates the recorded voltage pulse, is integrated over in a time window of 40 ns, which ensures full coverage of the waveform. Dividing the integrated waveform (in units  $V \cdot s$ ) by the impedance of the oscilloscope ( $50 \Omega$ ) leads to the charge (in C). Dividing the charge by the electron charge  $e = 1.6 \cdot 10^{-19} \text{ C}$  yields the number of electrons.

$$G_{1pe} = \frac{1}{e} \cdot \frac{\int V dt}{50 \Omega}$$

The intensity of the LED is chosen such that, on average, less than one photon is detected. Assuming Poisson statistics, for  $\mu_{\text{Poisson}} \ll 1$ , the recorded spectrum consists then primarily of the pedestal peak (0 pe), the single pe and a small contribution of 2 and more pe's (see Figure 7). The calibration spectrum was fitted with a sum of two Gaussian distributions; the centre of the second one corresponds to  $G_{1pe}$ . The value was found to be  $\approx 35 \text{ pV} \cdot \text{s}$ , or expressed in electrons:  $4.375 \cdot 10^6 \text{ e}$ .

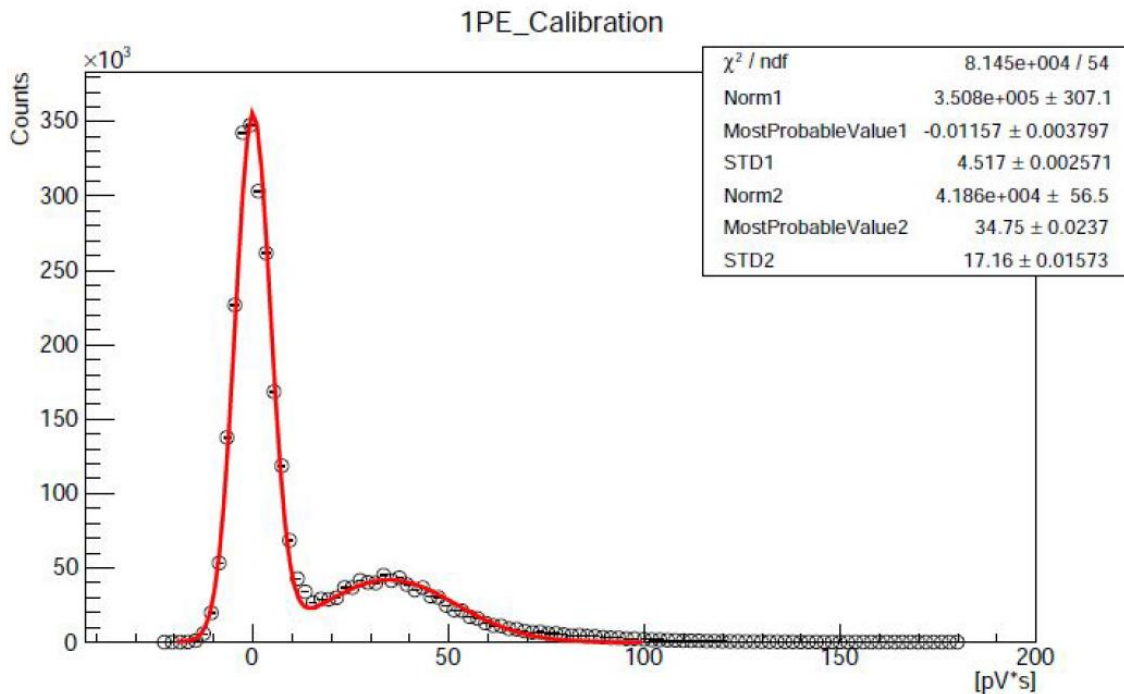


Figure 7: Single photoelectron calibration

### 3. Data Analysis

Figure 8 : Example of a charge spectrum from a light yield measurement on 3 standard SCSF-78 fibres, at 90 cm distance from the PMT. The average signal obtained via the COG method is 156 pV·s, corresponding to 4.5 pe.

The analysis can be performed in two ways:

- **Centre-of-gravity (COG) method:** The average of the histogram is determined, while ignoring the pedestal peak. Due to the non-perfect separation of the signal from the pedestal, the signal is assumed to decrease linearly to zero under the pedestal, which makes a small correction to the result. Alternatively and more precisely, the pedestal is first fitted by a root program and subtracted from the measured distribution, leaving the signal-only part. Integration and division of the average by the above determined  $G_{1pe}$  leads to the average number of signal photons detected from the fibres under test. The COG method has the advantage that it is robust also for small signals.

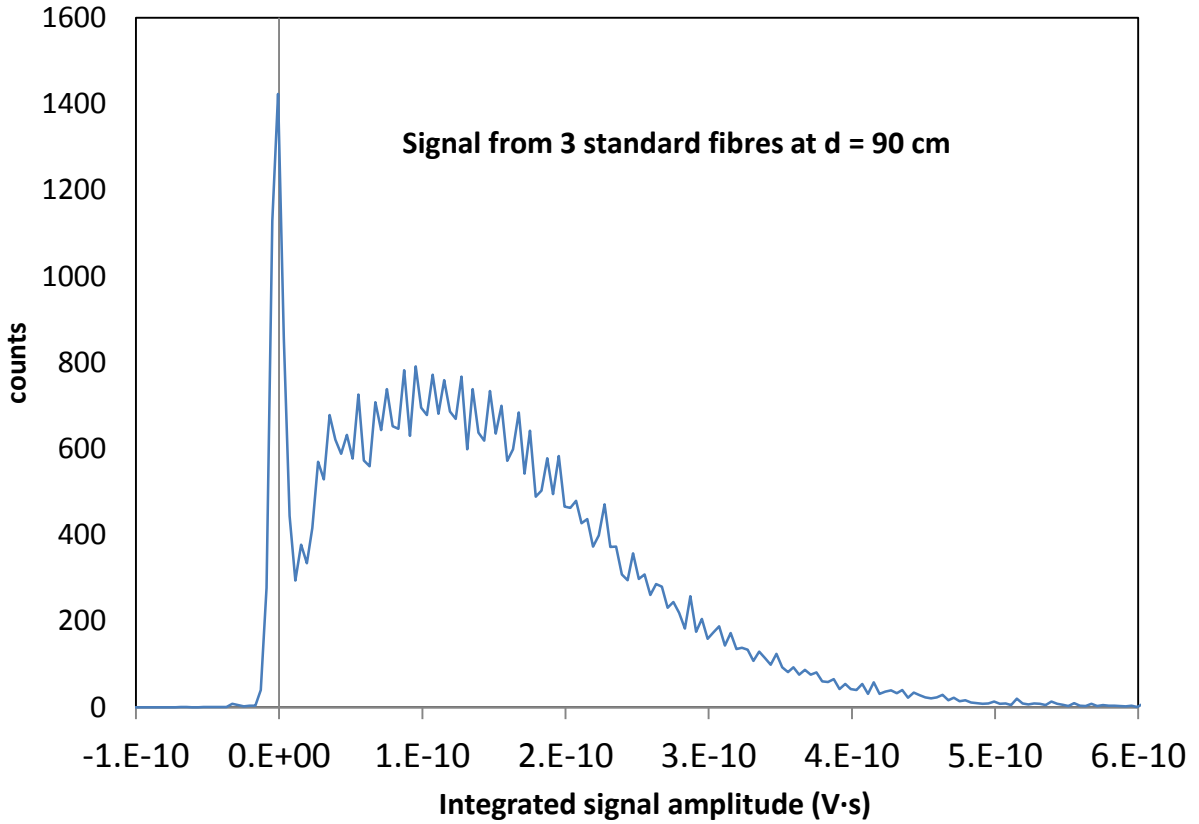


Figure 8 : Example of a charge spectrum from a light yield measurement on 3 standard SCSF-78 fibres, at 90 cm distance from the PMT. The average signal obtained via the COG method is 156 pV·s, corresponding to 4.5 pe.

- **Statistical Method:** With the knowledge of the single photoelectron distribution, the shape of the signal spectrum can be described by a sum of Gaussians  $G$  weighted by a Poisson distribution  $P$ . The corresponding fit function contains the parameter  $N_{pe}$ , the average of the Poisson distribution, which is the only free parameter to be determined by the fit.

$$C(Q; N_{pe}) = \int_0^r \sum_{k=1}^r P(k, N_{pe} * L(x)) * G \left( \text{Gain} * k, \sqrt{k * \sigma_{1pe}^2 + \sigma_{ped}^2} \right) dx$$

Here,  $\sigma_{1pe}$  and  $\sigma_{ped}$  are the variances of the pedestal peak and of the 1 photoelectron signal, respectively, determined from the calibration spectrum. The different effective path lengths  $L$  of the electrons in the fibre are taken into account in the fit function. They are estimated based on the assumption that the electrons traverse the fibres on parallel trajectories (see Figure 9).  $R$  is the fibre's radius and  $x$  ( $0 < x < R$ ) the impact parameter rel. to the fibre centre:

$$L(x) = \sqrt{R^2 - x^2}$$

The  $k = 0$  term (pedestal) cannot be included in the fit, as the pedestal is also due to the imperfect alignment of triggers and signal fibres. The statistical model fails to work for small signals (with an average below approx. 1 pe), because with the absence of the pedestal information, the parameter  $N_{pe}$ , cannot be reliably determined anymore.

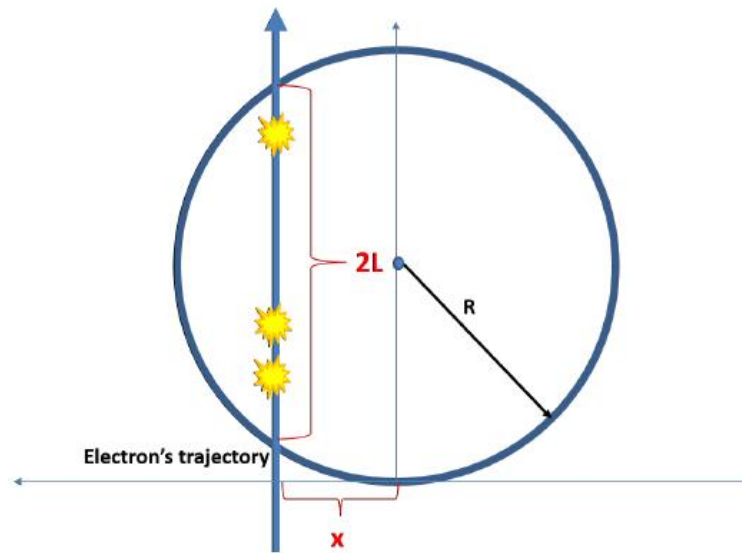


Figure 9: Example of an electron trajectory through the fibre.

## 4. Results and discussion

Figure 10 shows as an example the yield results for 3 different fibre sample as a function of the distance from the photodetector. The data sets can be described with single exponential fits, provided the data points at 60 cm and below are excluded. At these relatively short distances the light transport through non-core modes becomes noticeable and would require a second shorter exponential term. We take as scintillation yields the extrapolation of the exponential terms to  $d = 0$ .

The above described measurement of the scintillation yield involves manual manipulation of very small diameter fibres. This leads unavoidably to small variations in the fibre positioning from measurement to measurement. Repetition of measurements with the same fibres showed reproducibility of the result within 10%. All SCSF-78 fibre samples, provided by Kuraray as reference samples for the novel NOL fibres (SCSF-L1,2), were found to show equal light yield well within 10%.

Efforts are ongoing to describe the scintillation yield and attenuation effects by means of a microscopic simulation code, originally developed at the University of Dortmund. The results will be documented in a forthcoming note.

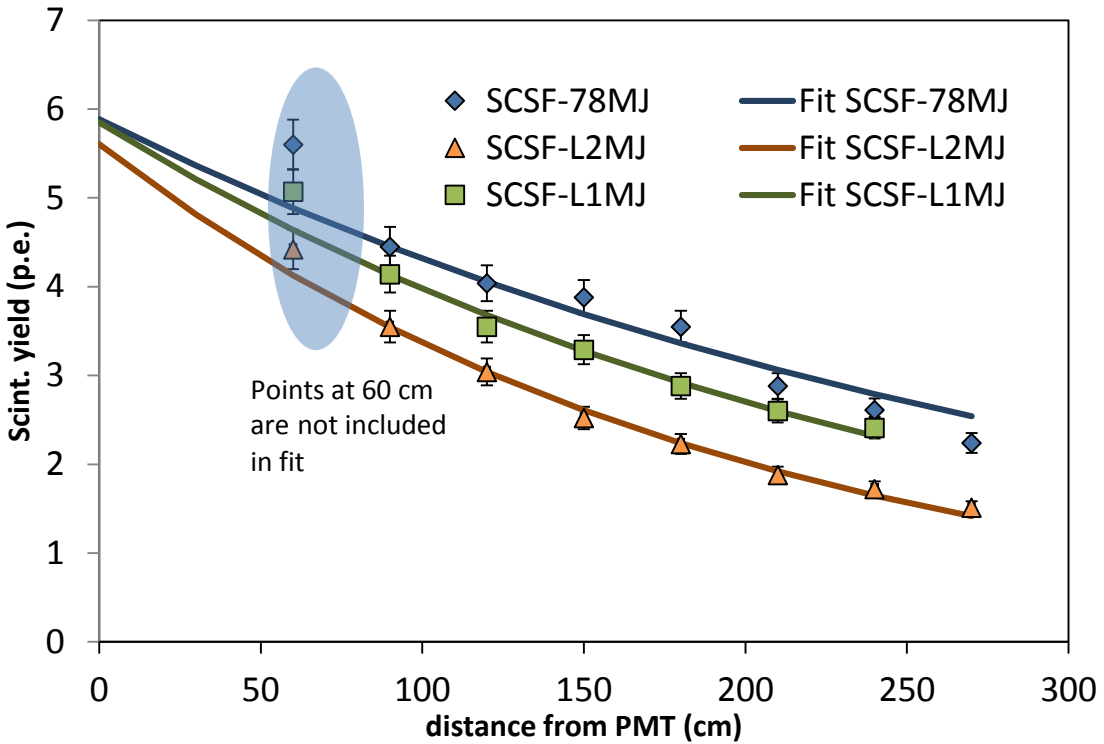


Figure 10 : Summary of light yield measurements on a different fibre samples. The yields are for arrangements of 3 fibres, jointly read out. Two of the 3 samples are newly developed NOL samples, which are compared to SCSF-78 standard fibres.

## 5. Replacement of the signal PMT by a SiPM readout

Light Yield measurements of green emitting NOL prototype fibres suffered from an insufficient matching of the emission spectrum with the sensitivity of the bialkali PMT, which peaks (~20-25%) at 400 nm, but drops to 10-15% at 500 nm. A straightforward approach is the replacement of the PMT by a SiPM detector. The new generation of Hamamatsu SiPMs has a quasi-ideal Photon Detection Efficiency (PDE) spectrum, peaking at 450 nm (PDE > 40%), and decreasing only by a few % at 400 and 500 nm. Even at 600 nm, the PDE is still around 25%.

The chosen SiPM is the Hamamatsu S13360-1350CS. Its  $1.3 \times 1.3 \text{ mm}^2$  active area is just large enough for the readout of a stack of 3 fibres which are bundled in a pin-connector with a  $\varnothing 0.7 \text{ mm}$  hole. The fibres need to be well centred on the SiPM, because the light spot exiting the fibre under angles of up to  $46^\circ$  (in air) is widening up when it traverses the 0.5 mm thick silicone resin entrance window.

The SiPM features 667 micro cells of  $50 \times 50 \text{ mm}^2$  size, guaranteeing perfect linearity in the range of interest (10 – 20 p.e.). Due to an efficient optical trench technology the SiPM is operated at typically 3 V overvoltage with a practically invisible cross talk of 1%. At this overvoltage, it reaches a gain of  $1.5 \cdot 10^6$ .

The SiPM is biased and read out via the driver circuit C12332-01, provided by Hamamatsu. It features a temperature-compensating bias supply (USB programmable) and a reasonably fast amplifier (fixed gain of 20,  $f_c = 40 \text{ MHz}$ ). For shielding of high frequency noise, the SiPM and its circuit are mounted in

a metal box, which at the same time acts as light shield. The light is fed into the box by a simple custom designed feedthrough which is centred on the SiPM.

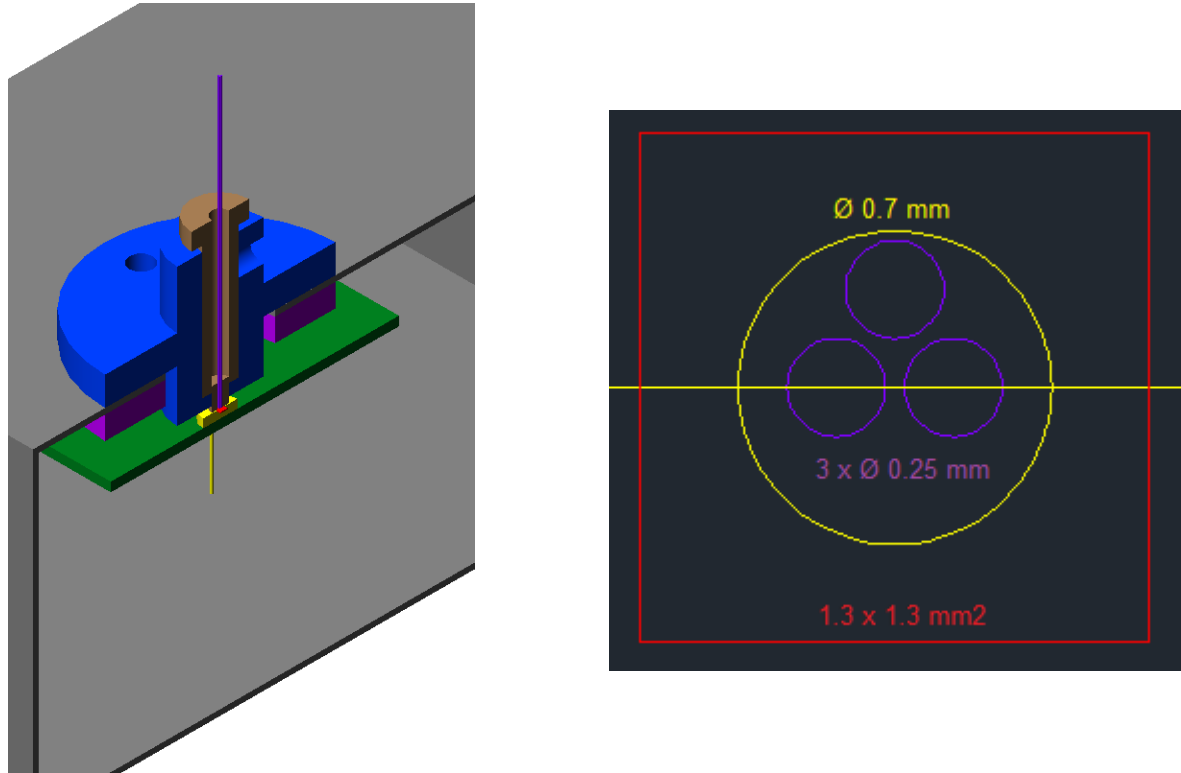


Figure 11 : Cut-through visualisation of the feedthrough (left) and the geometrical matching of the 3-fibre bundle to the active surface ( $1.3 \times 1.3 \text{ mm}^2$ ) of the SiPM (right). The fibres (violet) are randomly placed inside the yellow circle, which corresponds to the inner diameter of the fibre connector.

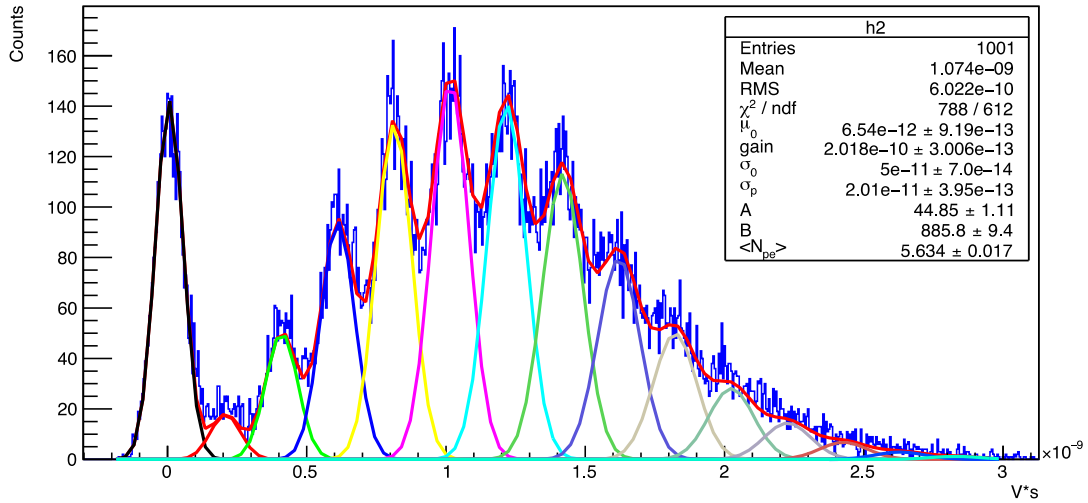


Figure 12 : Example of a SiPM calibration charge spectrum obtained with a pulsed LED light source.

A baseline instability of about  $\pm 1\text{mV}$ , modulated in the multi-kHz range, was observed at the output of the C12332 card (incl. factor 20 amplification), which spoiled the achievable resolution. The

problem could be significantly mitigated by processing the signal with an Ortec 474 shaping amplifier (differentiation time constant = 20 ns), before sampling it with the digital oscilloscope.

Figure 12 shows a typical SiPM multiphoton spectrum, obtained by exciting the 3 fibres by a pulsed fast LED (PicoQuant PLS370). The trigger for the acquisition is synchronous with the UV light pulse from the LED. The spectrum is well described by a convolution of a Poisson distribution (mean  $N_{pe}$ ) and a set of Gaussians (with correspondingly increasing width). In the fit, the pedestal peak at 0 is rescaled to account for geometrical inefficiencies (e.g. UV photon not hitting the fibres). From the distance of the peaks, the charge gain can be evaluated, which was found in this case to be 202 pVs/pe.

Figure 13, left, shows a charge spectrum obtained from a set of 3 standard fibres (SCSF-78, lot 151116-03). The peak structure allows to verify the charge gain of the photoelectrons. In principle, a dedicated calibration as shown in Figure 12 is no longer required. The large pedestal peak is from events which generate valid triggers, however do not deposit any detectable energy in the fibres (cladding, imperfect alignment). After fitting and adjusting the pedestal peak to  $Q=0$ , the spectrum is integrated from  $Q = 3\sigma_{ped}$  to the maximum recorded values (right plot). In the example below, a mean  $N_{pe}$  of 7.5 is obtained. A correction is needed as the suppressed pedestal also includes physical  $Q=0$  events which would lower the integral. Assuming that the spectrum has Poissonian shape (which is only a rough approximation), the charge integral is reduced by the factor  $(1 - P_0(N_{pe})) = 1 - \exp(-N_{pe})$ . As these corrections range from -5% for  $N_{pe} = 3$  to  $-4 \cdot 10^{-5}$  for  $N_{pe} = 10$ , the introduced additional uncertainty is small.

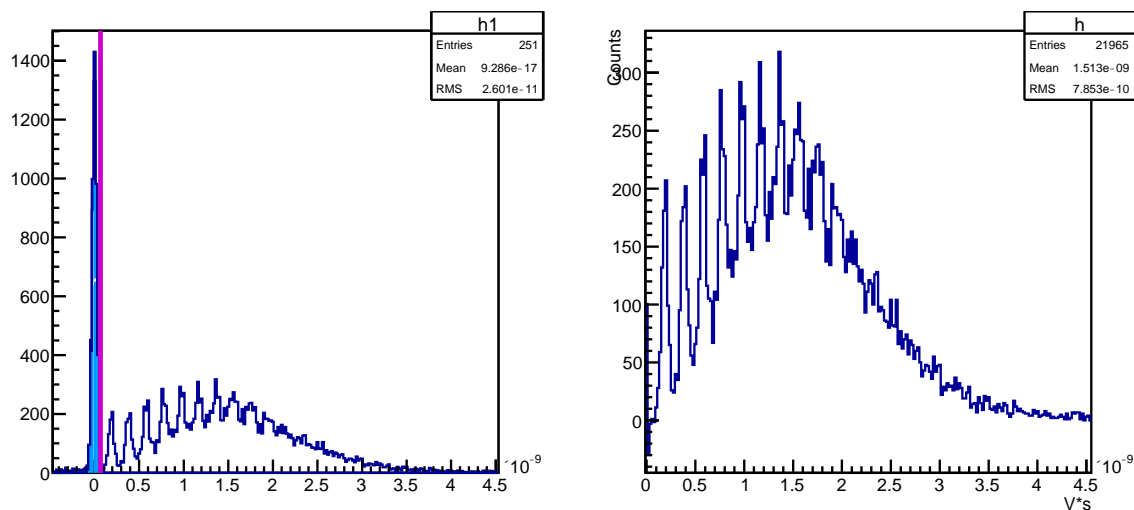


Figure 13 : Left: Example of a charge spectrum obtained with a set of 3 standard SCSF-78 fibres. Right: After pedestal subtraction.

Figure 14 shows an example of a light yield determination with the new SiPM readout system. A set of 3 standard fibres (SCSF-78, lot 151116-03) has been measured at distances between 90 and 240 cm. The extrapolation of the exponential fit to  $d=0$  leads to light yield of 13.9 pe.

### Uncertainties

A typical measurement at a given distance consists of taking 20'000 to 25'000 events. The statistical uncertainty of the integral (after pedestal subtraction), is calculated by ROOT and found to be of the order 3%.

Two series of dedicated measurements were performed to estimate the systematic uncertainties of the yield determination.

1. Repetitive measurements when removing and re-positioning the set of 3 fibres on top of the Sr-90 source. The introduced uncertainty, which is independent for the measurements at different distances, was found to be 1% (RMS). This uncertainty is therefore added in quadrature to the above mentioned statistical error.
2. Repetitive measurements when removing, rotating and re-inserting the fibre endpiece to the SiPM box. The related uncertainty was found to be 2.5% (RMS). This uncertainty is added linearly to the yield error given by the exponential fit for the whole dataset.

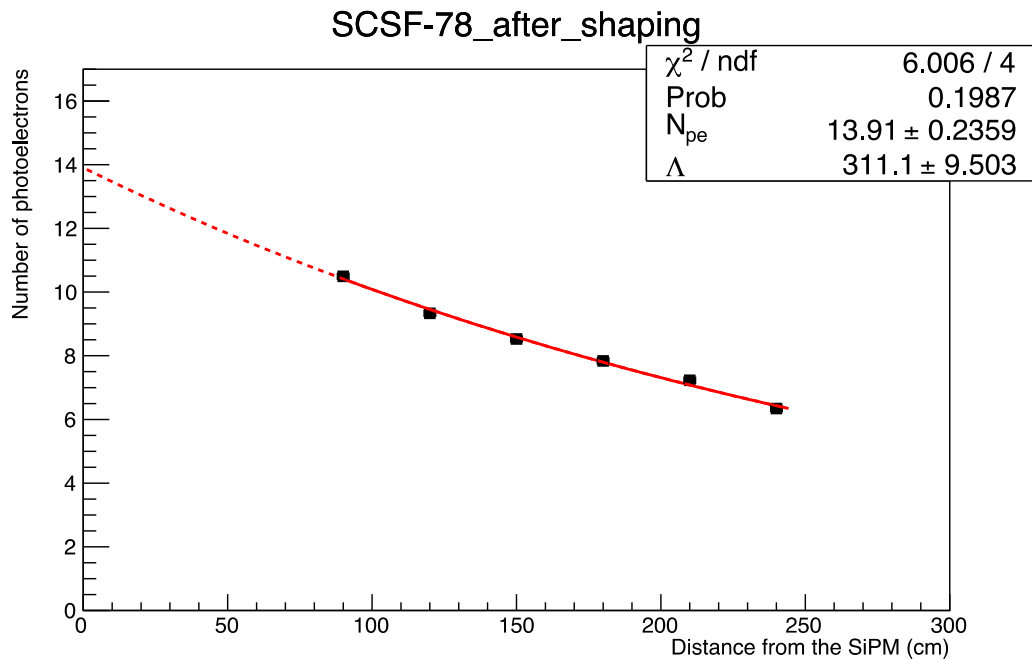


**Figure 14 : Measurement of the light yield of a set of 3 SCSF-78 standard fibres. The error bars are hidden by the symbols. The extrapolation of the exponential fit leads to a light yield of  $13.9 \pm 0.23$  pe. Adding the 2.5% uncertainty due to the endpiece positioning, the error becomes 0.58 pe.**

### Summary and conclusion

The new SiPM readout method profits from higher PDE and better spectral coverage. The high gain and small gain fluctuations allow for a precise gain calibration, even without dedicated calibration measurements. In addition, the PDE spectrum of the S13360 SiPM comes close to the PDE of the SiPM arrays intended to be used for the SciFi readout. This makes the light yield results and in particular the comparison between standard and NOL fibres even more significant as performance indicators for the use in the SciFi detector.

## Acknowledgements

We acknowledge Thomas Schneider, Miranda Van Stenis, Claude David and Francois Garnier for their precious suggestions and the production of the mechanical pieces; CERN Radioprotection service for its assistance in the  $^{90}\text{Sr}$  source's installation.

## References

1. LHCb collaboration, LHCb Tracker Upgrade, TDR, CERN/LHCC 2014-001
2. S. Arfaoui, C. Joram, C. Casella, Characterisation of a Sr-90 based electron monochromator, CERN PH-EP-Tech-Note-2015-00